DEMONSTRATING THE POTENTIAL OF ALOS PALSAR BACKSCATTER AND INSAR COHERENCE FOR FOREST GROWING STOCK VOLUME ESTIMATION IN CENTRAL SIBERIA

Christian Thiel, Christiane Schmullius

Department for Earth Observation, Friedrich-Schiller University Jena, Loebdergraben 32, 07743 Jena, Germany,
E-Mail: Christian.Thiel@uni-jena.de, C.Schmullius@uni-jena.de

ABSTRACT

The full potential of ALOS PALSAR L-band interferometric (InSAR) coherence data for the estimation of forest growing stock volume (GSV) in the boreal forest has rarely been investigated. Moreover, ALOS PALSAR backscatter and InSAR coherence have yet to be used together to delineate GSV. Due to the observation strategy and the high acquisition success rate over Eurasia, a large amount of high quality ALOS PALSAR L-band data is available over Siberia. Consequently, this paper investigates the capability of ALOS PALSAR backscatter and InSAR coherence for the estimation of GSV in Central Siberia, Russia. The potential of backscatter and coherence are directly compared using the same inventory data. Altogether, 87 PALSAR images are used and eleven forest inventory sites are investigated. Based on this large dataset it was observed that InSAR coherence acquired in frozen conditions offers the highest potential for GSV estimation. The saturation level for single coherence images was on average 230 m³/ha, with an average R² between coherence and GSV of 0.58. PALSAR backscatter acquired in unfrozen conditions could also estimate GSV; however, the saturation levels (75–100 m³/ha) and the average R² (0.42–0.48) were lower. HV backscatter offered only a slightly greater potential than HH backscatter.

1. INTRODUCTION

Much effort is spent on the assessment of the impact of human activities on the climatic change. Main sources of anthropogenic greenhouse gases emissions are from industry, transportation and agriculture. Beside these sources, about 20% of the CO_2 emissions also stem from deforestation or forest degradation. Therefore, it is necessary to quantify the amount of carbon bound in living forest biomass or GSV. Due to high temporal dynamics and large forest cover extent, ground based inventories are hardly capable to provide reliable estimates of carbon stock. Additionally, estimations of biomass/GSV from field data can have high uncertainties, as these parameters are typically estimated from field samples, not direct measurements. The integration of earth observation (EO) techniques can help to reduce uncertainties as spatial and temporal coverage are improved. EO techniques have already been applied to map forest cover extent, as well as changes in forest cover caused by clear-cut logging and forest fires. Current EO techniques applied for the estimation of forest stem volume still struggle with problems related to saturation and considerable uncertainties.

Thanks to the sophisticated observation strategy and the high acquisition success rate (approximately 80% over Eurasia), a large amount of high quality ALOS PALSAR L-band data is available over Siberia. Consequently, this paper investigates the potential of the PALSAR dataset, including backscatter and InSAR coherence, for GSV mapping in this region. Although a number of L-band based studies exist, the following issues, which are part of this research, have not yet been addressed previously:

i) Investigation of the potential of ALOS PALSAR HH and HV backscatter for GSV mapping in Central Siberia in frozen and unfrozen conditions,

ii) Direct comparison of L-band backscatter and InSAR coherence concerning the potential for GSV mapping (frozen and unfrozen conditions) for the same sites,

iii) Synergistic implementation of backscatter and InSAR coherence (magnitude) from the sensor ALOS PALSAR (temporal consistency and availability of the data) for the generation of maps with continuous GSV values.

iv) Detection and exclusion of areas where backscatter and InSAR coherence generated dissimilar results to improve the accuracy of the final map.

2. STUDY AREA

The study area is located in Central Siberia, Russia (Figure 1) and includes parts of the administrative compartments Irkutsk Oblast and Krasnoyarsk Kray. It is sited in the Middle Siberian Plateau, which is characterised by moderate topography, with elevations up to 1,700 m in the southern part. The northern part is rather flat with heights of less than 500 m. Mixed taiga forests (birch, pine, fir, aspen, larch, spruce, and cedar) cover approximately 80% of the region. Central Siberia exhibits extreme continental climatic conditions. The yearly amount of precipitation is generally below 450 mm. Most of the precipitation generally occurs between long dry periods during the summer, while most winters are rather dry with average temperatures considerably below 0°C. The whole territory is characterised by forest cover disturbances caused by forest fires, insect outbreaks and logging.
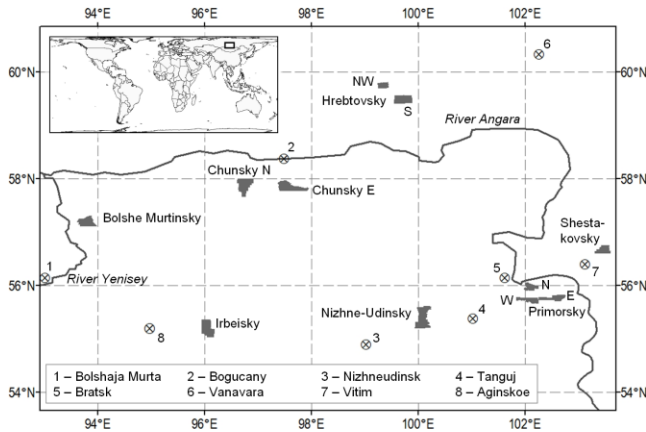
Figure 1. Study area in Central Siberia including forest inventory sites and weather stations (numbered). Each of the sites contains more than 330 forest stands. All sites together comprise 12,243 stands. Excluding clear-cuts, the average GSV is 185 m³/ha which corresponds to a tree height of 18 m.

3. DATA

3.1. Forest Inventory Data

Forest inventory data were available for a number of local sites. This work comprises the sites Bolshe Murtinsky NE, Chunsky N and E, Primorsky N, E, and W, Hrebtovsky S, and NW, Nishne Udinsky, Irbeisky, and Shestakovsky (Figure 1), as these sites feature a wide range of GSV values (see Table 2), which are relevant for a meaningful empirical data analysis, as well for the training of the empirical models. Each of the sites comprises more than 330 stands. All sites together comprise 12,243 stands. The average stand size is approximately 20 ha with a standard deviation of 11.6 ha. The data contain a multitude of parameters including stand ID, stand age, GSV, and relative stocking.

3.2. Meteorological Data

Meteorological data were collected for the stations Bolshaja Murta, Bogucany, Nizhneudinsk, Tanguj, Bratsk, Vanavara, Aginskoe and Vitim (Figure 1). All meteorological data were gathered from the global World Meteorological Organization (WMO) weather station network. Temperature, precipitation, wind, and snow depth was assembled for the acquisition date of the SAR data. Regarding precipitation, a sum of the past 3 and 7 days prior the acquisition was collected.

In general, during the winter the temperatures were below the freezing point and snow accumulated on the ground. During the summer, the temperatures were above 0°C. Winter SAR acquisitions featuring thaw were omitted in this work. Thaw was declared, when the minimum temperatures exceeded the freezing point. Thaw/refreeze events in between acquisitions were no exclusion criterion.

At no time was heavy rain reported during the SAR acquisitions. The maximum amount of precipitation was 8 mm per day. At most acquisition dates, no precipitation was observed. Wind data were also collected. As wind conditions can change quickly, the measurement time must not significantly deviate from the SAR data acquisition time. However, in some cases, wind and SAR acquisition differed more than 10 hours. Apart from that, the measured wind speeds were mostly close to zero with a maximum of 7 m/s.

3.3. ALOS PALSAR Data

Table 1 summarises the PALSAR data used in this study. Although the investigation was carried out for 11 local sites, only eight frames were required, as some of the frames cover more than one site.

Table 1. PALSAR data. *Cursive: unfrozen*; **Bold: FBD**; Other: FBS & frozen, T=track, F=frame

Location	Chunsky N	Chunsky E	Primorsky	Bolshe
Track	T475	T473	T466	T481
Frame	F1150	F1150	F1110	F1140
2006		30 Dec 06		28 Dec 06
2007	*20 Jun. 07*	14 Feb. 07	18 Jan. 07	12 Feb. 07
	5 Aug. 07	*2 Jul. 07*	5 Mar. 07	*15 Aug. 07*
	20 Sep. 07	*17 Aug. 07*	*21 Jul. 07*	*30 Sep. 07*
	5 Nov. 07	*2 Oct. 07*	*5 Sep. 07*	31 Dec. 07
	21 Dec. 07	*17 Nov. 07*	*21 Oct. 07*	
2008	5 Feb. 08	2 Jan. 08	21 Jan. 08	15 Feb. 08
	22 Mar. 08	17 Feb. 08		*2 Jul. 08*
	7 May 08	*4 Jul. 08*		*17 Aug. 08*
	22 Jun. 08	*19 Aug. 08*		
	7 Aug. 08			
2009		4 Jan. 09		2 Jan. 09
		19 Feb. 09		17 Feb. 09

Location	Shesta.	Nizhne	Irbeisky	Hrebt.
Track	T0463	T0471	T0478	T0468
Frame	F1130	F1100	F1100	F1190
2006				
2007	13 Jan. 07	11 Jan. 07	*10 Aug. 07*	6 Jan. 07
	28 Feb. 07	26 Feb. 07	*10 Nov. 07*	21 Feb. 07
	16 Jul. 07	*14 Jul. 07*	26 Dec. 07	*9 Jul. 07*
	31 Aug. 07	*14 Oct. 07*		*24 Aug. 07*
	16 Oct. 07			*9 Oct. 07*
2008	16 Jan. 08	14 Jan. 08	10 Feb. 08	9 Jan. 08
	2 Mar. 08	29 Feb. 08	*27 Jun. 08*	24 Feb. 08
	17 Apr. 08	*16 Jul. 08*	*12 Aug. 08*	*11 Jul. 08*
	18 Jul. 08	*31 Aug. 08*	28 Dec. 08	*26 Aug. 08*
	2 Sep. 08			
2009	18 Jan. 09	16 Jan. 09	12 Feb. 09	11 Jan. 09
	5 Mar. 09	3 Mar. 09	*30 Jun. 09*	26 Feb. 09
	21 Jul. 09		*15 Aug. 09*	*14 Jul. 09*
	5 Sep. 09		*30 Sep. 09*	*29 Aug. 09*
	21 Oct. 09			*14 Oct. 09*

According to t*he PALSAR acquisition strategy*, fine beam single (FBS) polarisation data (HH) were acquired in winter (roughly November to March), and fine beam dual (FBD) polarisation data (HH, HV) were acquired in summer/autumn (roughly June to October). Altogether, 87 SLC images were used in this study (FBS: 40 images, FBD: 47 images). For the coherence estimation only the HH polarisation data were used. The azimuth pixel spacing of the SLC data is 3.15 m. The slant range pixel spacing is 4.7 m for FBS (28 MHz), and 9.4 m for FBD (14 MHz) data. Regarding interferogram processing, most image pair combinations were considered. Pairs featuring mixed conditions

(frozen and unfrozen), and pairs with $B_\perp$ (perpendicular baseline) exceeding the critical value were omitted.

All SAR data were delivered in JAXA's (Japan Aerospace Exploration Agency) level 1.1 format, referring to single look complex (SLC) data in slant range geometry. The backscatter processing steps comprised radiometric calibration, multilooking including intensity image calculation, 3 arcsec SRTM DEM based orthorectification and topographic normalisation. Interferometric processing includes SLC data co-registration to sub-pixel accuracy, slope adaptive common-band filtering in range direction to correct for geometric decorrelation and common-band filtering in azimuth direction. The interferograms were generated using 10×20 looks for FBS and 10×40 looks for FBD data.

4. METHODS

4.1. Data SAR Data Analysis to assess the Sensitivity of Backscatter and Coherence for GSV

All analyses were conducted at the forest stand level. Accordingly, backscatter and coherence were averaged for each forest stand. To summarise the observations, several statistics were estimated:

i) Average backscatter and coherence of non-forest (inventory data was used to extract all areas with a GSV of 0 m³/ha, i.e. non-forest),

ii) Average backscatter and coherence of dense forest (inventory data was used to extract all areas with a GSV between 250 m³/ha and 350 m³/ha, i.e. dense forest),

iii) GSV saturation level (the basic idea was to compute the separability of adjacent biomass classes (class width = 50 m³/ha) starting at the lowest GSV level),

iv) Coefficient of determination R^2 for predicted GSV estimates, using empirical exponential equations.

4.2. Integrative usage of SAR backscatter and coherence for the mapping of GSV

The approach of the delineation of the SAR based GSV maps can be outlined as follows (details are provided afterwards):

i.) Stratified random training data selection (20% of the forest inventory data),

ii.) Training of empirical models for HV backscatter and coherence data using least squares fitting,

iii.) Pixel based model inversion and GSV estimation,

iv.) Averaging HV backscatter and coherence GSV maps resulting in one backscatter and one coherence based GSV map,

v.) Merging the coherence and the HV backscatter GSV maps ((a) averaging, (b) elimination of areas featuring GSV difference greater 100 m³/ha, (c) setting negative values of averaged map to zero).

vi.) Assessing the accuracy of the final map using the remaining 80% of the reference data.

These six steps were applied to the sites Chunsky E, Chunsky N, Shesta, Hrebt S, and Nishni, because these sites had at least three HV backscatter images acquired in unfrozen conditions and three coherence images acquired in frozen conditions were also available.

5. RESULTS

5.1. Data SAR Data Analysis to assess the Sensitivity of Backscatter and Coherence for GSV

In total, 87 ALOS PALSAR acquisitions were used and approximately 300 coherence images were delineated for GSV estimation. With regard to coherence, only the results being potentially relevant for GSV estimation are presented here. This includes the coherence images acquired in frozen conditions (0 m $< B_\perp <$ 1,800 m, no exclusion of interferogram based on $B_\perp$) and the coherence images acquired in unfrozen conditions with 3,100 m $< B_\perp <$ 4,100 m. Regarding the latter, it was found that the PALSAR coherence data with $B_\perp <$ 2,000 m was not sensitive enough for estimating GSV. The impact of $B_\perp$ on coherence over sparse and dense forest was investigated in a previous study using the same data. In frozen conditions, no impact was observed for 0 m $< B_\perp <$ 1,800 m. In unfrozen conditions, a slight impact between 1,000 m and 2,000 m was observed. Therefore, no subgroups featuring different perpendicular baselines were formed for this study. The majority of the coherence images had a temporal baseline of 46 days. The maximum temporal baseline was 138 days. Larger temporal baselines were omitted in order to avoid heavy temporal decorrelation. The same applies to interferograms employing data from dissimilar seasons (i.e. one image acquired in unfrozen conditions, and one image acquired in frozen conditions).

In the following, the observations of all considered SAR data are summarised for all eleven inventory sites. Figure 2 provides a graphical presentation of the major observations. In these four diagrams, the first three columns show the coherence data. The remaining four columns display the results based on the backscattering intensity.

All results are subdivided into frozen and unfrozen conditions. Due to the lack of an adequately dense network of meteorological stations, a further subdivision considering more detailed environmental conditions was not feasible. Regarding the backscatter data, the polarisations HH and HV were distinguished. Regarding coherence, the group frozen conditions were subdivided into two partitions to account for the increasing impact of temporal decorrelation. The first partition contains the interferograms with a temporal baseline of 46 days; the second partition features temporal baselines of 92 and 138 days. For unfrozen conditions, only interferograms with a temporal baseline of 46 days were used.

(a) Signatures of clear-cuts

(c) Correlation of GSV and SAR data

(b) Signatures of dense forest

(d) GSV saturation level

● = average; ⊥ = standard deviation; ⁻ = minimum/maximum
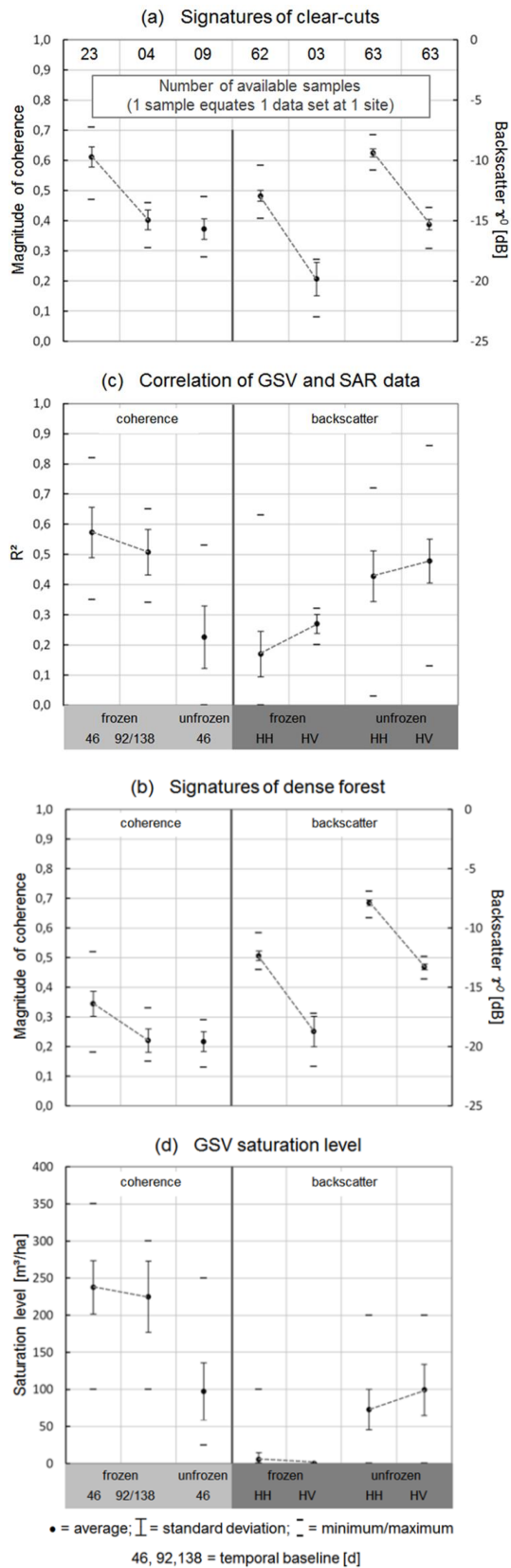
46, 92,138 = temporal baseline [d]

Figure 2. Summarised results of the PALSAR data analysis for evaluating the potential regarding GSV estimation including INSAR coherence and backscatter, both acquired

in frozen and unfrozen conditions. Provided are (a) the average signatures of clear-cuts, (b) the average signatures of dense forest, (c) the correlation of GSV and SAR parameter, and (d) the saturation for GSV. The statistics are separated by season, temporal baseline, and polarisation. See (a) for the number of samples. One sample refers to one backscatter/coherence image at one forest inventory site, thus each sample comprises 339-2046 forest stands.

Figure 2 (a) summarises the backscatter and the coherence of clear-cuts, i.e. areas with a GSV of 0 m²/ha. Therefore, low backscattering intensity and high coherence values can be expected. Diagram (b) presents the backscatter and coherence for dense forest (250-350 m³/ha), thus high backscatter and low coherence can be expected. Commonly, the magnitude of the difference between the SAR signatures of dense forest and non-forest is related to the potential for GSV estimation: larger differences often coincide with a higher potential for GSV retrieval.

Coherence acquired in frozen conditions with a temporal baseline of 46 days had the largest contrast between open areas and dense forest. The highest coherence over open areas was observed for frozen conditions with a temporal baseline of 46 days. The average value was 0.61. Dense forests had an average coherence of 0.34. In this example, the difference between open areas and dense forest was 0.27. With increasing temporal baseline the coherence decreased over both open areas and dense forest. A reduced difference of 0.19 was also observed. Given unfrozen conditions, the coherence over dense forest and open areas was similar to the coherence acquired in frozen conditions with temporal baselines of 92/138 days.

Contrary to coherence, the largest contrast of backscatter between open areas and dense forest was observed in unfrozen conditions. This contrast decreased in frozen conditions. For example, a backscattering difference of 0.2 dB in frozen and of 2.0 dB in unfrozen conditions was observed for HH polarisation. A 5.0 dB drop in backscatter was detected for dense forest in HH polarised images during frozen conditions. The drop was even larger for HV polarisation (6 dB). In open areas, the backscatter also decreased during frozen conditions. However, this decrease was not as large as in dense forest (HH: 3 dB, HV: 4.5 dB).

The highest R^2 values (0.51-0.58) were found for coherence acquired in frozen conditions (Figure 4 (c)). Also, there was a slight decrease of R^2 values for the large temporal baseline. The R^2 for backscattering intensity acquired in unfrozen conditions ranged from 0.42 (HH) to 0.48 (HV). The HV polarisation had a noticeably wide range of the R^2 values (0.13 to 0.87; Figure 2 (c)). For the majority, the average R^2 values of the remaining SAR data were overall very low. Coherence acquired in unfrozen conditions and backscatter acquired in frozen conditions were in general not useful for GSV estimation. Roughly the same conclusions were drawn regarding the saturation level. Saturation was reached on average between 200 m²/ha and 250 m²/ha. The saturation of the backscattering intensity

was reached at considerably lower GSV levels of 75 m²/ha for HH and at 100 m²/ha for HV data. Coherence acquired in unfrozen conditions had a saturation level of 100 m²/ha. In summary, coherence acquired in frozen conditions demonstrated the greatest potential for GSV estimation. It had the highest R² and the highest saturation levels. In comparison to other studies based on L-band coherence data, higher saturation levels were identified in this study. The backscattering intensity acquired in unfrozen conditions also demonstrated some potential to estimate GSV; however, it suffers from a comparably low saturation level. Still, the radar backscatter might be useful to improve a coherence based GSV product, as discussed above in this section. The joint application of backscattering intensity and coherence for GSV estimation is demonstrated in the following paragraph.

5.2. GSV mapping results

In the following the GSV map for Hrebtovsky S (Figure 3) as well as the accuracy statistics for the other four chosen test sites derived using the procedure described in section 4.2 are discussed. For the delineation of the GSV map, three coherence images and six HV backscatter images were available. The average R² between coherence and GSV was 0.44. This value is rather low when compared to Figure 2 (c). The saturation level was determined at 250 m³/ha. The average R² between HV backscatter and GSV was 0.48, which corresponds quite well to the average of all investigated sites. The HV backscatter was found to saturate at 200 m³/ha, which is a high value compared to the average of 100 m³/ha (Figure 2).
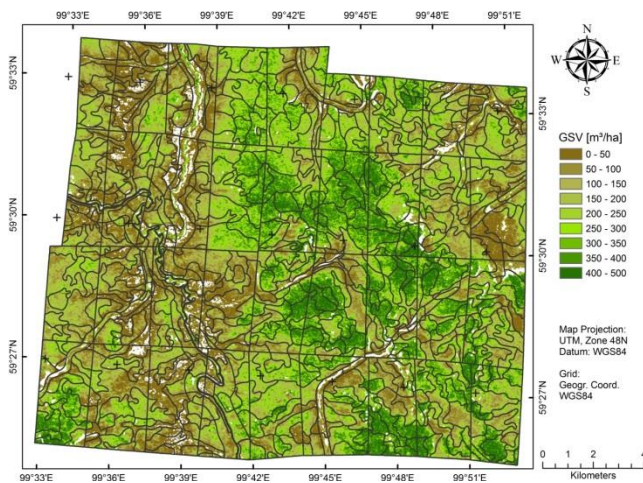

Figure 3. GSV map of Hrebtovsky S based on 6 HV backscatter images acquired in unfrozen conditions and 3 HH coherence images acquired in frozen conditions. Information on the accuracy is provided in Figure 4 (b). White areas refer to no-data. The polygons encircle the forest stands.

It was observed in the GSV map (Figure 3) that patches featuring no-data (referring to eliminated data, see section 4.3) were primarily found next to areas with a low GSV, which was usually located in floodplains. One potential reason for this observation is the high sensitivity of the SAR backscatter to soil moisture during unfrozen conditions. In particular, the soil moisture in floodplains is typically high, sometimes they are even flooded. Therefore, high backscatter can occur in areas with sparse forest. During frozen conditions, the impact of soil moisture changes is reduced, which would explain why a high coherence was found. On the other hand, decorrelation can be caused by forest management activities taking place in open areas such as clear-cuts. These activities may include the transportation of wood, the removal of debris or the installation of local infrastructure for the forestry management sector. Although this kind of change causes decorrelation, the impact on the backscatter can be rather low. By eliminating areas that have a GSV difference between the backscatter and coherence based GSV map greater than 100 m³/ha, some errors related to the above issues can be avoided.

The accuracy of the final maps was evaluated with the remaining 80% of the reference data. For this step, R² and RMSE were computed. To be precise, the RMSE should be treated as root mean square deviation between forest inventory data and the SAR based GSV map, as the inventory data itself has an $RMSE_{inv}$ of 15% - 20%.

There was generally good agreement between forest stand level GSV derived from backscatter and coherence when compared to the forest inventory GSV data (Figure 4 (a)). An overall bias was not observed. For the comparison of GSV estimates of backscatter to coherence data, an R² of 0.79 was found and a relative RMSE of 25% was observed. The averaging of backscatter and coherence GSV maps helped to reduce the spread at low GSV levels. Yet, backscatter and coherence GSV were spread around the 1:1 line; meaning that the usage of either backscatter or coherence could introduce an under- or overestimation of GSV.

In comparison to the forest inventory, a marginal improvement in the proportion of variance (R² = 0.54) in GSV estimation accounted for by the combination of coherence and backscatter data was observed (Figure 4 (b)). This is relative to the individual performances of coherence (R² = 0.50) and backscatter (R² = 0.51) to estimate GSV. The relative RMSE of the combined data was 33%, which was slightly lower than observed individually for coherence (37%) and backscatter (36%) data. Thus, the synergistic usage of backscatter and coherence may not only be useful for determining exclusion criteria for areas with considerable GSV differences, but it may also have some potential to improve SAR-based GSV estimations.
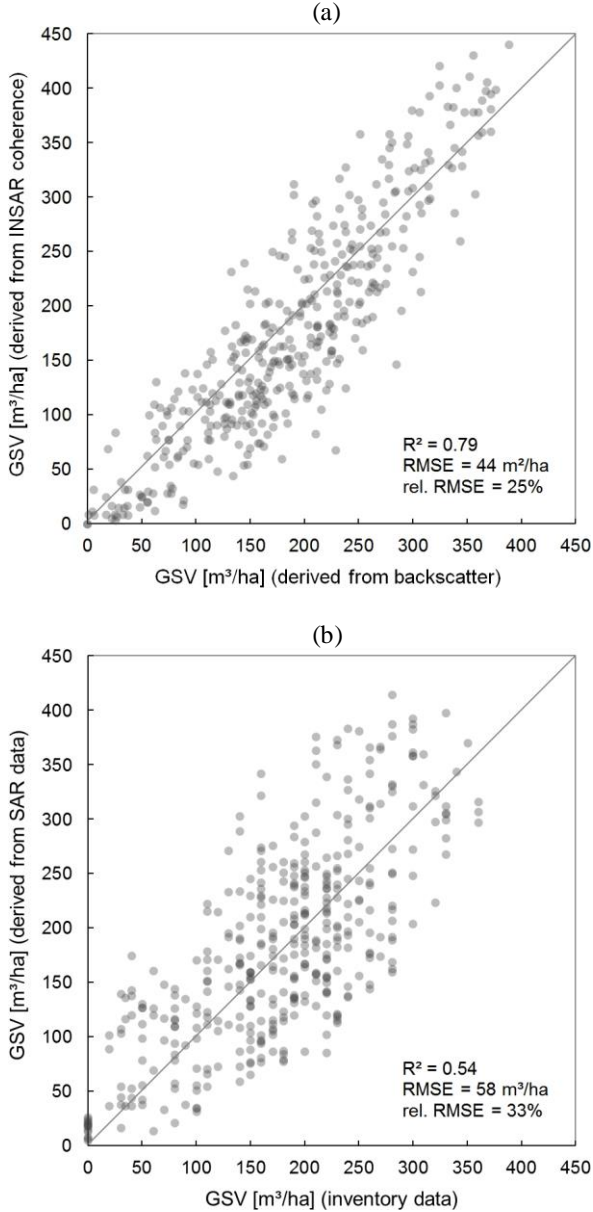
Figure 4. (a) Forest stand level based comparison of two SAR data based GSV maps for Hrebtovsky S; (b) Forest stand level based comparison of inventory data and the final SAR data based GSV map.

As reported above, the relative RMSE between inventory data and the final PALSAR based GSV was 33%. If independence is assumed for the SAR based estimation error $RMSE_{sar}$ and the inventory estimation error $RMSE_{inv}$, a corrected $RMSE_{corr}$ of the final PALSAR based GSV map can be computed: $RMSE_{corr} = (RMSE_{sar}^2 - RMSE_{inv}^2)^{0.5}$. Accordingly, the relative $RMSE_{corr}$ for Hrebtovsky S lies between 26% and 29%. Thus, the final PALSAR based map features an accuracy which was close to the accuracy of the forest inventory data. Compared to previous work in this field of science, this result corresponds to the studies reporting the higher accuracies.

Table 2 provides rel. $RMSE_{corr}$ and R^2 for all five sites. Except for Chunsky N, the rel. $RMSE_{corr}$ was below 30%. The reason for the rather high error value for Chunsky N lies in the comparably low average GSV of this site (a high percentage of Chunsky N was harvested or in some stage of regrowth), the absolute RMSE for Chunsky N was similar to the other sites.

Table 2. Accuracy assessment of the predicted GSV for the sites Chunsky E, Chunsky N, Shesta, Hrebt S, and Nishni.

	Chunsky E	Chunsky N	Shesta	Hrebt S	Nishni
No. of images backscatter/coherence	5/5	5/6	6/3	6/3	4/3
rel. $RMSE_{corr}$ [%]	59.0	29.8	28.5	26.0	28.3
R^2	0.79	0.79	0.54	0.57	0.83

6. SUMMARY AND CONCLUSIONS

The study investigates the capability of L-band backscatter and coherence for the estimation of GSV in Siberia using a large amount of PALSAR data. It was observed that coherence acquired in frozen conditions offers the largest potential for GSV estimation. For single images, the saturation occurs in average at 230 m³/ha, the R^2 between coherence and GSV was 0.58 on average. Comparable results were found in other studies using ERS 1/2 Tandem data. Results based on JERS 1 coherence had lower saturation levels. PALSAR backscatter also had some sensitivity to GSV estimation. However, saturation occurred at lower GSV levels (75-100 m³/ha). Also, the average R^2 was lower (0.42-0.48). Regarding L-band backscatter, slightly lower GSV saturation levels and coefficients of determination compared to other studies was observed. Overall, HV backscatter offered a slightly greater potential than HH backscatter for GSV estimation.

GSV maps were generated and validated for five sites. For the delineation of the map coherence data acquired in frozen conditions and backscatter data acquired in unfrozen conditions were used. The delineation was based on a rather simple and straight forward approach that could be operationally applied over large areas. This approach does not consider potential change within the time series of acquisitions. Areas featuring change such as new clear-cuts could be detected, e.g. by computing multitemporal metrics using the backscatter images. The training of the GSV retrieval algorithms was based on forest inventory data. One requirement of the conventional forest inventory data is that it comprises the whole range of appearing GSV levels. If no inventory data are available, the usage of other products, such as the MODIS Vegetation Continuous Fields, may be applied for the model training. Another successfully applied training approach is based on the analysis of the image statistics of SAR data.

In general, the produced maps feature a corrected relative $RMSE_{corr}$ of < 30%. This figure assumes an RMSE of 20% of the inventory data. Thus, the final PALSAR based map features an accuracy which is close to the accuracy of the forest inventory data itself. Compared to previous work in

this field of science, this result corresponds to studies reporting the higher accuracies.

The approach is based on a suited PALSAR data set with regard to the acquisition conditions. It was found that frozen conditions are crucial for qualifying InSAR coherence to be used as estimator for GSV. If meteorological data are available, the environmental conditions for the time of the acquisition time can be examined before data processing and unsuited image pairs can be avoided. For the case of meteorological data being unavailable the coherence data can be analysed, as image pairs acquired at dissimilar conditions (frozen/unfrozen) of a thaw event at one of the acquisition dates become manifest in significantly reduced coherence over open areas. Therefore, a straight forward strategy would be to exclude those image pairs by applying a coherence threshold for open areas.

In summary, it could be demonstrated that ALOS PALSAR data have the potential to map the GSV of the Siberian forest with an accuracy of the conventional forest inventory data. Thanks to the sophisticated observation strategy and the high acquisition success rate in that area, on average four coherence images (temporal baseline 46 days) for each site in Siberia were acquired in frozen conditions and six FBD backscatter images acquired in unfrozen. The results of this study might gather some particular importance with regard to ESA's forthcoming earth explorer mission BIOMASS, as for a great partition of the boreal zone (Northern America, Northern Europe) P-band acquisitions may not/or only partly be permitted.

This work was published 2016 in detail in the Journal of Remote Sensing of Environment. For the full publication please see [1].

7. ACKNOWLEDGEMENT

8. REFERENCES

1. C. THIEL & C. SCHMULLIUS (2016): The potential of ALOS PALSAR backscatter and InSAR coherence for forest growing stock volume estimation in Central Siberia images.-In: Remote Sensing of Environment 173, pp. 258-273.